ELSEVIER

Journal of Volcanology and Geothermal Research 120 (2002) 43–53

Journal of volcanology and geothermal research

www.elsevier.com/locate/jvolgeores

# U–Pb zircon chronostratigraphy of early-Pliocene ignimbrites from La Pacana, north Chile: implications for the formation of stratified magma chambers

Axel K. Schmitt [a,*], Jan M. Lindsay [b], Shan de Silva [c], Robert B. Trumbull [d]

[a] *Department of Earth and Space Sciences, UCLA, Los Angeles, CA 90095-1567, USA*
[b] *Seismic Research Unit, University of the West Indies, St. Augustine, Trinidad and Tobago*
[c] *Department of Space Studies, University of North Dakota, Grand Forks, ND USA*
[d] *GeoForschungsZentrum, Potsdam, Germany*

Received 15 October 2001; accepted 30 January 2002

**Abstract**

High spatial resolution U–Pb dates of zircons from two consanguineous ignimbrites of contrasting composition, the high-silica rhyolitic Toconao and the overlying dacitic Atana ignimbrites, erupted from La Pacana caldera, north Chile, are presented in this study. Zircons from Atana and Toconao pumice clasts yield apparent $^{238}U/^{206}Pb$ ages of $4.11 \pm 0.20$ Ma and $4.65 \pm 0.13$ Ma ($2\sigma$), respectively. These data combined with previously published geochemical and stratigraphic data, reveal that the two ignimbrites were erupted from a stratified magma chamber. The Atana zircon U–Pb ages closely agree with the eruption age of Atana previously determined by K–Ar dating ($\sim 4.0 \pm 0.1$ Ma) and do not support long ($>1$ Ma) residence times. Xenocrystic zircons were found only in the Toconao bulk ignimbrite, which were probably entrained during eruption and transport. Apparent $^{238}U/^{206}Pb$ zircon ages of $\sim 13$ Ma in these xenocrysts provide the first evidence that the onset of felsic magmatism within the Altiplano–Puna ignimbrite province occurred approximately 3 Myr earlier than previously documented.


*Keywords:* La Pacana caldera; stratified magma chamber; ignimbrite; rhyolite; U/Pb; zircon

## 1. Introduction

It is widely accepted that a spectrum of processes operate to produce compositional diversity in silicic magma systems, but their relative importance is debated (Eichelberger et al., 2000, 2001; de Silva, 2001). Evidence for crystal–liquid separation is nearly ubiquitous (e.g. Smith, 1979; Hildreth, 1981). Recharge, where transiently distinct magma batches are juxtaposed immediately prior to eruption, may be important in some systems (e.g. Eichelberger and Izbekov, 2000; Schmitt et al., 2001). Since both models are based on studies of heterogeneous pyroclastic deposits, elucidating the roles of these mechanisms depends critically on detailed and precise volcanic chronostratigraphy.

* Corresponding author. Tel.: +1-310-794-5047; Fax: +1-310-825-2779.
*E-mail address:* axel@argon.ess.ucla.edu (A.K. Schmitt).

0377-0273/02/$ – see front matter 
PII: S0377-0273(02)00359-1

Stratigraphic and geochemical evidence suggested that two huge compositionally contrasting ignimbrites, the Atana and Toconao ignimbrites (combined volume ~2700 km$^3$), erupted from La Pacana caldera in the Central Andes and that they are consanguineous and represent separate layers of a stratified magma (Lindsay et al., 2001a,b). However, the temporal relations between the two units were ambiguous since previous K–Ar dating yielded inconclusive and, in part, geologically unreasonable ages (see review in Lindsay et al., 2001a). The abundance of xenolithic material and scarcity of datable materials in the crystal-poor Toconao ignimbrite rendered conventional dating methods ineffective. Recent success in ion microprobe dating of Pliocene–Pleistocene zircons (e.g. Baldwin and Ireland, 1995; Brown and Fletcher, 1999; Dalrymple et al., 1999; Reid and Coath, 2000) established ion microprobe $^{238}U/^{206}Pb$ dating as a promising tool for unraveling the history of young pyroclastic systems. Here we demonstrate that $^{238}U/^{206}Pb$ dating of zircons yields insights into the crystallization history of the two La Pacana ignimbrites. U–Pb zircon geochronology indicates a close temporal relationship between the Toconao and Atana magmas and, in combination with petrological data from La Pacana, challenges the view that compositional gaps in pyroclastic deposits are in general best explained by incomplete mixing between magmas of different origin (e.g. Eichelberger et al., 2000). We suggest instead that stratification in the La Pacana system developed due to effective crystal-melt separation within an upper-crustal magma reservoir and that the layers continued to evolve independently after separation.

## 2. Geologic background of La Pacana caldera

One of Earth's most extensive silicic volcanic provinces is the Altiplano–Puna Volcanic Complex (APVC), located between 21 and 24°S in the Central Andes (de Silva, 1989a). Here, at least 30 000 km$^3$ of late-Miocene to Pleistocene ignimbrites and silicic lavas are preserved above a zone of extremely low S-wave velocities at mid-crustal depths that probably represents a partially molten magma body of cordilleran batholith proportions (e.g. Chmielowski et al., 1999; Haberland and Rietbrock, 2001). Previous studies suggested that ignimbrite activity in the APVC started at ~10 Ma and reached its peak between approximately 7 and 3 Myr ago with the caldera-forming eruptions of La Pacana in north Chile (Gardeweg and Ramírez, 1987; de Silva, 1989b) and of Pastos Grandes, Cerro Guacha and Cerro Panizos in south Bolivia (Francis and Baker, 1978; Ort, 1993).

The Toconao and Atana ignimbrites are both distributed around and thicken towards La Pacana caldera (Lindsay et al., 2001a; Fig. 1). The Toconao ignimbrite (180 km$^3$) comprises a thin (< 10 cm) lower fall unit with glassy crystal-poor (< 3%) tubular pumice and a thick (~30 m) upper flow unit and locally displays two facies that are caused by varying degrees of vapor-phase alteration. The overlying 2500 km$^3$ dacitic Atana ignimbrite is homogeneous, crystal-rich (40–50%), relatively pumice-poor, and constitutes a single cooling unit. The Atana intracaldera facies is densely welded, whereas degree of welding varies in extracaldera outcrops. There is no field evidence for a hiatus between deposition of the Toconao and the overlying Atana ignimbrite but previous geochronology is inconclusive as to the timing of the two eruptions. Two stratigraphically consistent whole-rock and biotite K–Ar ages were previously determined for Toconao pumice, these are 4.0 ± 0.9 and 5.27 ± 1.12 Ma (all errors 2σ, see Lindsay et al., 2001a). Recent K–Ar biotite ages from Atana pumice have generally smaller uncertainties and range between 3.77 ± 0.09 Ma and 4.23 ± 0.12 Ma (Lindsay et al., 2001a).

## 3. Methods

Zircons were recovered by heavy liquid separation from the < 350-μm fraction from three samples used for K–Ar dating by Lindsay et al. (2001a): Atana single pumice (Lari-96h-6), Toconao bulk ignimbrite (Quis-96-3), and a Toconao single pumice clast (Toc-97h-2) collected at the same location (Fig. 1) as the composite pumice sample (Toc-97h-3) dated by Lindsay et al.

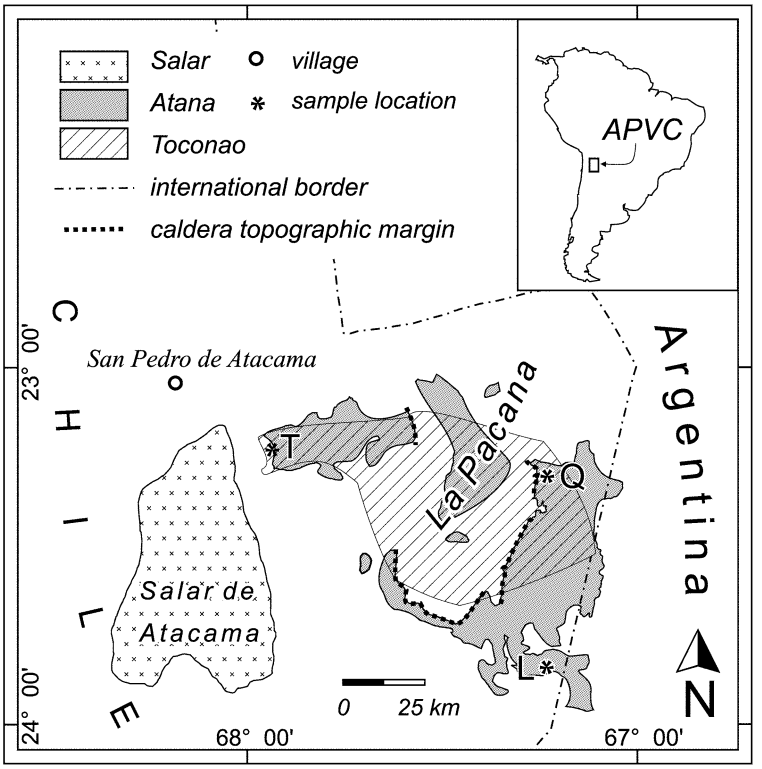


Fig. 1. Map of La Pacana Caldera in the APVC showing the distribution of Atana ignimbrite and the estimated extent of the underlying Toconao ignimbrite (modified after Lindsay et al., 2001b). Sample locations for K–Ar and U–Pb zircon dating are indicated (T = Toc-97h-2; Q = Quis-96-3; L = Lari-96h-6).

(2001a). Lithic clasts are abundant in the bulk ignimbrite sample, but were separated by hand-picking prior to crushing and sieving. Prior to ion probe analyses, a total of ~50 polished zircons was examined for internal zonation by cathodoluminescence (CL) imaging (Fig. 2).

Ion microprobe spot analyses were performed using the UCLA CAMECA ims 1270 ion microprobe on all zircons recovered from the two Toconao samples (~10 each) and on 11 selected grains from the Atana sample. A 5–10-nA $O^-$ primary beam was focused to a spot size of ~30 μm in diameter (see Fig. 2) and secondary ions extracted at 10 kV with an energy band pass of 35 eV. $O_2$ pressure in the sample chamber was adjusted to ~0.002 Pa to increase Pb sensitivity. The reproducibility on the reference zircon AS3 (Paces and Miller, 1993) during the three analytical sessions between March and August 2001 varied between 1 and 3%. To determine the age of the outermost zones, rim analyses were performed on one unpolished Toconao zircon grain using the depth-profiling mode, which improves the spatial resolution by a factor of ~100 (c.f. Grove and Harrison, 1999). Fig. 3 and Table 1 show increasing radiogenic $^{206}Pb$ coupled with decreasing $^{207}Pb/^{206}Pb$ ratios for four successive analyses on an unpolished crystal face. This implies that common Pb is largely surface derived and therefore a 5-min pre-sputtering was applied during analyses on polished surfaces.

## 4. Results

A $^{204}Pb$-based common Pb correction can introduce large uncertainties for young unradiogenic samples and therefore the uncorrected data (analytical results shown in Table 1) were regressed in the $^{238}U/^{206}Pb$ vs. $^{207}Pb/^{206}Pb$ diagram to ob-

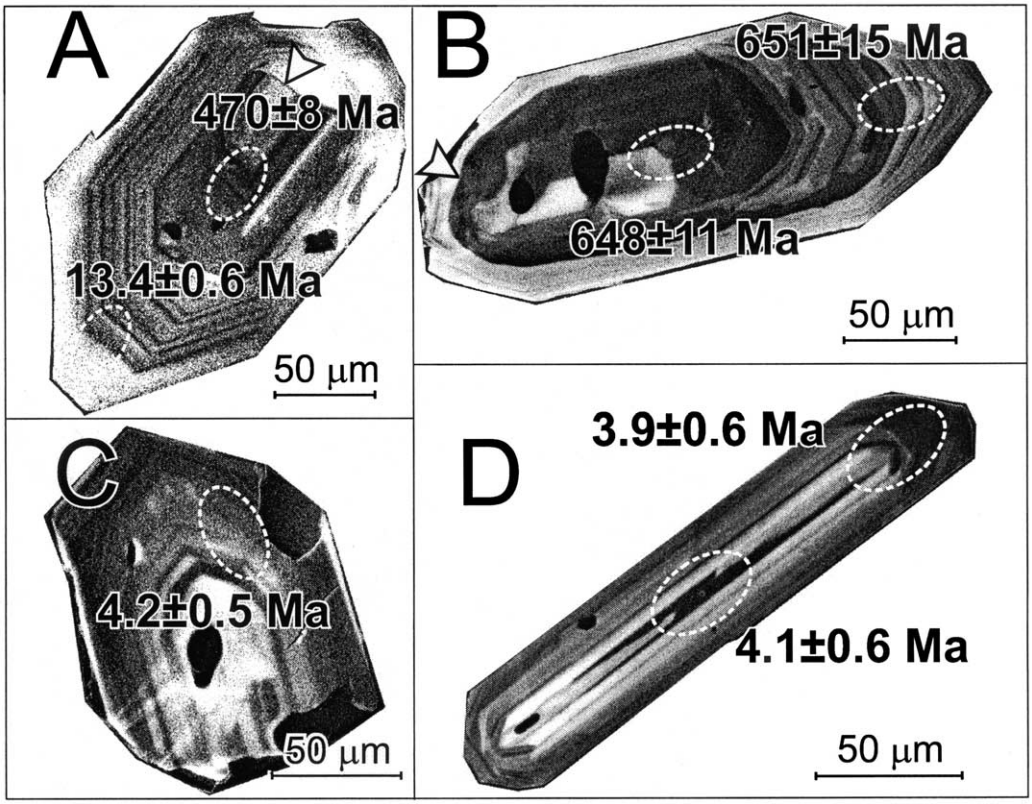


Fig. 2. CL images of zircons from La Pacana. Ion microprobe spots are indicated by dashed line together with $^{204}$Pb-corrected ages (1σ errors). Arrows indicate truncation of oscillatory zonation. (A) Toconao bulk ignimbrite Quis-96-3 grain 11. (B) Grain 2 from same sample. (C) Toconao pumice Toc-97h-2 grain 7. (D) Atana pumice Lari-96h-6 grain 5.

tain apparent ages from the intercept with concordia and common $^{207}$Pb/$^{206}$Pb compositions from the *y*-axis intercept (Fig. 3). Table 2 summarizes the apparent $^{238}$U/$^{206}$Pb ages from the concordia intercept method and the averages of the $^{204}$Pb-corrected ages. Both approaches yield apparent ages that overlap within error, but the intercept method has the advantage that no additional assumption on the $^{206}$Pb/$^{204}$Pb ratio of the common Pb has to be made. In the following sections, we therefore report and discuss only apparent ages yielded by the concordia intercept method.

A 4.65 ± 0.13 Ma (mean square of weighted deviates (MSWD) = 1.1) age is obtained for the Toconao pumice from regression of depth-profile and polished-surface analyses (including one core analysis on the same grain that was used for depth-profile analysis). The corresponding $^{207}$Pb/$^{206}$Pb composition of non-radiogenic lead is 0.75 ± 0.09. U contents in Toconao pumice zircons are estimated to range between ~400 and ~1200 ppm and most analyses on polished surfaces yielded radiogenic $^{206}$Pb > 90% (Table 1).

All zircons from the Toconao bulk ignimbrite sample yielded considerably older U–Pb ages that greatly exceed the range of existing K–Ar ages for Toconao and violate the stratigraphic constraints. Three of the 10 grains yielded concordant Proterozoic to Ordovician ages (Fig. 2; Table 1). CL imaging shows truncation of oscillatory banding in the core of a forth grain (Fig. 2A). A concordant 470 ± 9 Ma core age and a ~13 Ma rim age would be consistent with resorption of an inherited Ordovician grain and subsequent Miocene overgrowth although we note that similar trunca-

tions are also present in grains in which core and rim analyses yield overlapping Proterozoic ages (Fig. 2B). The U–Pb data for the Miocene overgrowth zone and six other grains from the bulk ignimbrite sample plot close to 13 Ma and 9 Ma reference lines in Fig. 3.

U–Pb data of zircons from Atana pumice define a regression line, which yields a concordia intercept age of 4.11 ± 0.20 Ma (MSWD = 2.6, $^{207}Pb/^{206}Pb = 0.80 \pm 0.08$). Atana zircons have estimated U contents between ~200 and ~1100 ppm and despite their complex internal zoning (Fig. 2C,D) $^{204}Pb$-corrected core and rim ages overlap within error. The apparent age derived from Atana zircons agrees well with previously published biotite K–Ar ages on three aliquots of the same sample (3.94 ± 0.12, 4.01 ± 0.11 and 4.11 ± 0.12 Ma, Lindsay et al., 2001a), and is slightly but significantly lower than the age obtained from Toconao zircons.

## 5. Pre-eruptive residence time and stratigraphy of consanguineous, compositionally contrasting magmas

The analyzed Atana zircon population yields stratigraphically consistent apparent ages that overlap with the K–Ar biotite ages for Atana samples, which are interpreted as eruption ages. We interpret the zircon U–Pb ages as crystallization ages due to the low diffusivity of Pb in crystalline zircon even at magmatic temperatures (Cherniak and Watson, 2000). The apparent $^{238}U/^{206}Pb$ ages reported in Table 2 likely represent minimum ages, since a $^{230}Th$ deficit caused by preferential incorporation of U compared to Th has to be expected during zircon crystallization (Mattinson, 1973; Schärer, 1984). The calculated age correction for initial $^{230}Th$ deficit in the Toconao and Atana samples using Th/U in whole rocks (Lindsay et al., 2001b) and zircon is +80 kyr and +90 kyr, respectively. Unless one assumes extremely strong inhibition of $^{206}Pb$ accumulation (e.g. by loss of $^{222}Rn$), even the disequilibrium-corrected ages are difficult to reconcile with long (>1 Ma) pre-eruptive crystal residence times. Such long residence times were postulated for

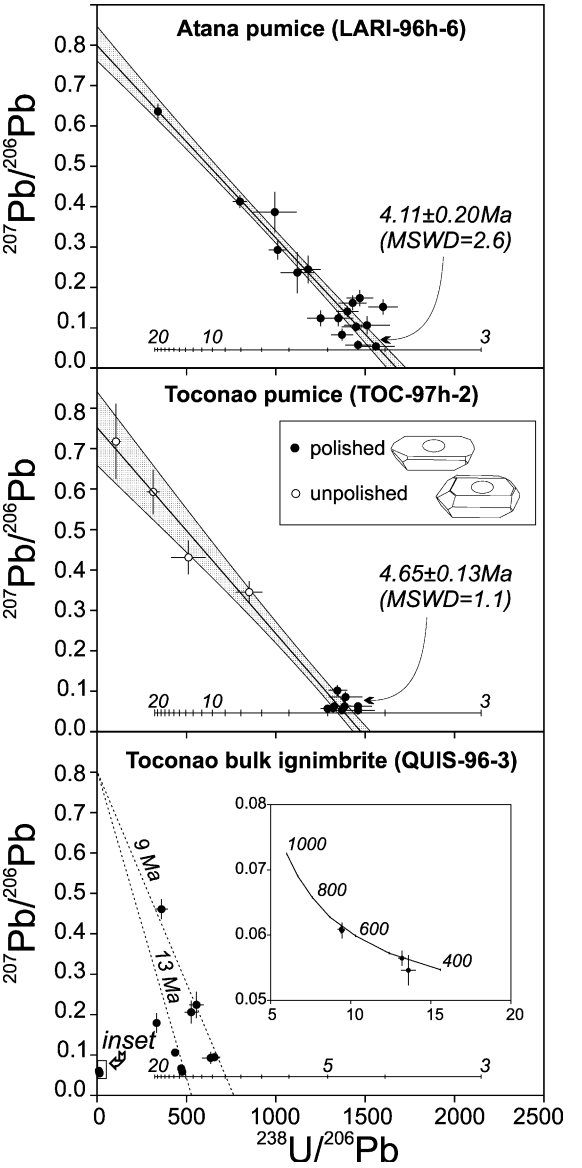


Fig. 3. U–Pb ion microprobe results for La Pacana zircons uncorrected for common Pb (1σ errors). Values for concordia are illustrated between 3 and 20 Ma, and 400 and 1000 Ma (in inset); linear regression lines and 2σ-error envelopes were plotted for sample Lari-96h-6 and Toc-97h-2. 9-Ma and 13-Ma-reference isochrons in lower panel were drawn using an average $^{207}Pb/^{206}Pb$ ratio of 0.8 for common Pb. MSWD = mean square of weighted deviates.

the Bishop Tuff (van den Bogaard and Schirnick, 1995; Christensen and Halliday, 1996) but later challenged by Reid and Coath (2000) on the grounds of ion microprobe U–Pb zircon dating.

Table 1
U–Pb ion microprobe results for zircons from La Pacana, north Chile

| Sample | Grain | Spot | Remarks[a] | $^{206}Pb/^{238}U$ | $^{206}Pb/^{238}U$ | $^{207}Pb/^{235}U$ | $^{207}Pb/^{235}U$ | error correlation | $^{207}Pb/^{206}Pb$ | $^{207}Pb/^{206}Pb$ | % radiogenic $^{206}Pb$ | Age[b] (Ma) | ± Age (Ma) | Age[b] (Ma) | ± Age (Ma) |
|---|---|---|---|---|---|---|---|---|---|---|---|---|---|---|---|
| | | | | | 1σ | | 1σ | | | 1σ | | $^{238}U/^{206}Pb$ | $^{238}U/^{206}Pb$ | $^{207}Pb/^{206}Pb$ | $^{207}Pb/^{206}Pb$ |
| *Atana pumice* | | | | | | | | | | | | | | | |
| Lari-96h-6 | 2 | 1 | core | 0.000846 | 0.000051 | 0.02850 | 0.00516 | 0.77 | 0.245 | 0.034 | 41.7 | 2.27 | 0.75 | – | – |
| Lari-96h-6 | 2 | 2 | rim | 0.000893 | 0.000075 | 0.02922 | 0.00833 | 0.88 | 0.237 | 0.051 | 81.4 | 4.61 | 0.76 | – | – |
| Lari-96h-6 | 3 | 1 | core | 0.000681 | 0.000035 | 0.01629 | 0.00248 | 0.76 | 0.174 | 0.020 | 91.9 | 4.04 | 0.25 | – | – |
| Lari-96h-6 | 3 | 2 | rim | 0.000626 | 0.000032 | 0.01308 | 0.00206 | 0.75 | 0.152 | 0.019 | 88.8 | 3.58 | 0.22 | – | – |
| Lari-96h-6 | 3 | 3 | rim | 0.000690 | 0.000039 | 0.00983 | 0.00139 | 0.62 | 0.103 | 0.012 | 90.5 | 3.83 | 0.39 | – | – |
| Lari-96h-6 | 5 | 1 | core | 0.001251 | 0.000062 | 0.07130 | 0.00538 | 0.88 | 0.413 | 0.016 | 50.2 | 4.05 | 0.59 | – | – |
| Lari-96h-6 | 5 | 2 | rim | 0.000803 | 0.000048 | 0.01375 | 0.00277 | 0.82 | 0.124 | 0.019 | 74.9 | 3.90 | 0.61 | – | – |
| Lari-96h-6 | 6 | 1 | rim | 0.000712 | 0.000032 | 0.01380 | 0.00170 | 0.72 | 0.141 | 0.013 | 90.4 | 4.15 | 0.24 | – | – |
| Lari-96h-6 | 6 | 2 | core | 0.000742 | 0.000046 | 0.01266 | 0.00234 | 0.56 | 0.124 | 0.020 | 76.5 | 3.59 | 0.51 | – | – |
| Lari-96h-6 | 8 | 1 | core | 0.001006 | 0.000123 | 0.05368 | 0.01155 | 0.84 | 0.387 | 0.050 | 54.4 | 3.53 | 1.02 | – | – |
| Lari-96h-6 | 8 | 2 | rim | 0.000732 | 0.000033 | 0.00842 | 0.00144 | −0.06 | 0.083 | 0.015 | 100.0 | 4.58 | 0.28 | – | – |
| Lari-96h-6 | 13 | 1 | core | 0.002940 | 0.000118 | 0.25770 | 0.01389 | 0.83 | 0.636 | 0.019 | 31.5 | 3.88 | 1.39 | – | – |
| Lari-96h-6 | 18 | 1 | core | 0.000701 | 0.000038 | 0.01569 | 0.00235 | 0.76 | 0.162 | 0.019 | 86.5 | 3.91 | 0.26 | – | – |
| Lari-96h-6 | 19 | 1 | core | 0.000995 | 0.000050 | 0.04021 | 0.00488 | 0.87 | 0.293 | 0.024 | 67.9 | 4.35 | 0.53 | – | – |
| Lari-96h-6 | 25 | 1 | core | 0.000685 | 0.000034 | 0.00548 | 0.00120 | 0.37 | 0.058 | 0.012 | 100.0 | 4.19 | 0.33 | – | – |
| Lari-96h-6 | 26 | 1 | core | 0.000664 | 0.000057 | 0.00981 | 0.00193 | 0.04 | 0.107 | 0.023 | 84.5 | 3.45 | 0.74 | – | – |
| Lari-96h-6 | 30 | 1 | core | 0.000641 | 0.000043 | 0.00482 | 0.00098 | 0.20 | 0.055 | 0.011 | 91.8 | 3.58 | 0.46 | – | – |
| *Toconao pumice* | | | | | | | | | | | | | | | |
| TOC-97h-2 | 7 | 1a | rim[c] | 0.009527 | 0.002406 | 0.94310 | 0.24260 | 0.87 | 0.718 | 0.093 | 11.7 | 9.32 | 10.19 | – | – |
| TOC-97h-2 | 7 | 1b | rim[c] | 0.003184 | 0.000368 | 0.26050 | 0.04614 | 0.88 | 0.593 | 0.056 | 14.2 | 3.40 | 4.13 | – | – |
| TOC-97h-2 | 7 | 1c | rim[c] | 0.001957 | 0.000372 | 0.11620 | 0.02502 | 0.89 | 0.431 | 0.042 | 46.5 | 7.30 | 4.28 | – | – |
| TOC-97h-2 | 7 | 1d | rim[c] | 0.001175 | 0.000102 | 0.05584 | 0.00595 | 0.68 | 0.345 | 0.027 | 72.6 | 6.17 | 1.55 | – | – |
| TOC-97h-2 | 7 | 1e | core | 0.000721 | 0.000049 | 0.00847 | 0.00141 | 0.38 | 0.085 | 0.013 | 94.9 | 4.21 | 0.48 | – | – |
| TOC-97h-2 | 2 | 1 | rim | 0.000730 | 0.000039 | 0.00530 | 0.00104 | 0.33 | 0.053 | 0.010 | 80.9 | 3.54 | 0.59 | – | – |
| TOC-97h-2 | 2 | 2 | core | 0.000736 | 0.000027 | 0.00962 | 0.00116 | 0.27 | 0.095 | 0.011 | 94.3 | 4.68 | 0.31 | – | – |
| TOC-97h-2 | 3 | 1 | core | 0.000756 | 0.000030 | 0.00602 | 0.00066 | 0.23 | 0.058 | 0.006 | 100.0 | 4.15 | 0.36 | – | – |
| TOC-97h-2 | 4 | 1 | core | 0.000687 | 0.000037 | 0.00593 | 0.00090 | 0.29 | 0.063 | 0.009 | 100.0 | 4.43 | 0.24 | – | – |
| TOC-97h-2 | 4 | 2 | rim | 0.000752 | 0.000020 | 0.00628 | 0.00068 | 0.58 | 0.061 | 0.006 | 91.7 | 4.44 | 0.16 | – | – |
| TOC-97h-2 | 8 | 1 | core | 0.000683 | 0.000043 | 0.00495 | 0.00105 | 0.33 | 0.053 | 0.011 | 89.4 | 3.66 | 0.48 | – | – |
| TOC-97h-2 | 8 | 2 | rim | 0.000720 | 0.000018 | 0.00629 | 0.00054 | 0.36 | 0.063 | 0.005 | 95.5 | 4.43 | 0.14 | – | – |
| TOC-97h-2 | 9 | 1 | core | 0.000777 | 0.000024 | 0.00607 | 0.00070 | 0.24 | 0.057 | 0.006 | 97.4 | 4.87 | 0.24 | – | – |
| *Toconao tuff* | | | | | | | | | | | | | | | |
| Quis-96-3 | 1 | 1 | core | 0.002103 | 0.000099 | 0.01696 | 0.00114 | 0.74 | 0.058 | 0.003 | 98.8 | 13.4 | 0.6 | – | – |
| Quis-96-3 | 2 | 1 | core | 0.105800 | 0.001888 | 0.88110 | 0.02500 | 0.81 | 0.060 | 0.001 | 99.6 | 648 | 11 | 618 | 44 |
| Quis-96-3 | 2 | 2 | rim | 0.106300 | 0.002649 | 0.88820 | 0.02409 | 0.94 | 0.061 | 0.001 | 99.9 | 651 | 15 | 626 | 23 |
| Quis-96-3 | 3 | 1 | core | 0.003002 | 0.000121 | 0.07393 | 0.01210 | 0.76 | 0.179 | 0.024 | 85.3 | 16.7 | 0.9 | – | – |
| Quis-96-3 | 3 | 2 | core | 0.001525 | 0.000076 | 0.01984 | 0.00277 | 0.66 | 0.094 | 0.011 | 84.9 | 8.5 | 0.7 | – | – |
| Quis-96-3 | 4 | 1 | core | 0.002126 | 0.000094 | 0.01951 | 0.00199 | 0.58 | 0.067 | 0.006 | 97.0 | 13.4 | 0.7 | – | – |
| Quis-96-3 | 5 | 1 | core | 0.073290 | 0.002516 | 0.54660 | 0.03141 | 0.80 | 0.054 | 0.002 | 99.0 | 455 | 15 | 378 | 97 |
| Quis-96-3 | 6 | 1 | core | 0.001799 | 0.000134 | 0.05561 | 0.01152 | 0.88 | 0.224 | 0.033 | 73.9 | 8.9 | 0.9 | – | – |
| Quis-96-3 | 6 | 2 | core | 0.001575 | 0.000122 | 0.02014 | 0.00383 | 0.54 | 0.093 | 0.015 | 88.9 | 9.2 | 1.0 | – | – |
| Quis-96-3 | 7 | 1 | core | 0.001900 | 0.000133 | 0.05394 | 0.01033 | 0.85 | 0.206 | 0.028 | 83.7 | 10.3 | 0.9 | – | – |
| Quis-96-3 | 7 | 2 | core | 0.002778 | 0.000285 | 0.17650 | 0.02333 | 0.93 | 0.461 | 0.025 | 53.8 | 10.8 | 1.7 | – | – |
| Quis-96-3 | 11 | 1 | rim | 0.002291 | 0.000080 | 0.03355 | 0.00305 | 0.82 | 0.106 | 0.007 | 90.4 | 13.4 | 0.6 | – | – |
| Quis-96-3 | 11 | 2 | core | 0.075690 | 0.001414 | 0.58750 | 0.01688 | 0.89 | 0.056 | 0.001 | 99.6 | 470 | 8 | 465 | 46 |

[a] On polished surface (if not stated otherwise).
[b] After common Pb-correction using $^{206}Pb/^{204}Pb = 18.8$ and $^{207}Pb/^{204}Pb = 15.4$.
[c] Unpolished

Assuming that the Atana and Toconao magmas are consanguineous, we can estimate an average residence time in the order of ~500–750 kyr for the Toconao zircons, approximately two to three times longer than estimated for the Whakamaru ignimbrite, New Zealand (Brown and Fletcher, 1999). Note that these estimates scale proportional to the erupted volumes of the La Pacana (2700 $km^3$) and Whakamaru (1000 $km^3$; Brown and Fletcher, 1999) systems.

It has been argued that sharp gradients in chemical composition and intensive variables are difficult to reconcile with long-lived stratified magma chambers (Eichelberger et al., 2000). In the La Pacana case, however, the compositional gap between high-silica rhyolitic (~77 wt% $SiO_2$) Toconao and dacitic (68–70 wt% $SiO_2$) Atana bulk pumice is somewhat misleading since Atana glass is in fact high-Si rhyolite with compositions very similar to the Toconao bulk pumice (Table 2).

Furthermore, the equilibration pressures estimated for both magmas argue for storage at similar depth: pre-eruptive pressures for the Atana magma derived from Al-in hornblende barometry average 200 MPa (Lindsay et al., 2001b) whereas for the Toconao magma melt $H_2O$ contents of ~6 wt% were calculated using the plagioclase-melt equilibrium calibration of Housh and Luhr (1991) that correspond to a confining pressure of 200 MPa (Tamic et al., 2001). This, together with the chemical, isotopic and chronostratigraphic similarities of the two ignimbrites, weights heavily against the concept that the Toconao and the Atana magmas are unrelated and were fortuitously juxtaposed prior to the caldera-forming eruption.

The variations in volatile element abundances (e.g. Cl and B) with fractionation in melt inclusion glasses demonstrates that at least over the crystallization interval of quartz, the Atana magma was volatile saturated (Fig. 4). Gas-driven filter pressing has been postulated as an effective mechanism that facilitates segregation of residual melts from volatile-saturated, highly crystalline magmas (Sisson and Bacon, 1999) and could account for the co-existence of extremely crystal-poor and crystal-rich magmas within the same magma system. Comparison of Rb variations in the glass data also indicate that the Toconao magma segregated from the highly evolved Atana magma during this crystallization interval, and that differentiation of both Atana and Toconao magmas must have continued after their separation (Fig. 4). The slightly older age obtained from six Toconao zircons implies that zircon crystallization occurred diachronously within the La Pacana magma body. This would be consistent with a stratified rhyolite-over-dacite magma body in which zircon might start to crystallize earlier within a more rapidly cooled cupola zone and/or a compositionally more evolved high-silica rhyolite (Watson and Harrison, 1983). The absolute timing of rhyolite segregation, however, remains a matter for continued investigation since it cannot be ruled out that zircons in the Toconao pumice were brought along from the Atana source magma.

## 6. Xenocrystic zircon: evidence for an early onset of APVC magmatism and implications for source processes

Zircon grains with >5 Ma ages were found exclusively in the Toconao bulk ignimbrite sample. The ages violate the stratigraphic age of the Toconao ignimbrite and the most straightforward interpretation is that they represent xenocrysts incorporated during eruption and transport. Macroscopic lithic clasts were removed from the ignimbrite sample prior to crushing, but these clasts typically have a rounded appearance and thus it is likely that material derived from their edges became dispersed in the ignimbrite matrix. The most abundant type of lithic clast is a dense crystal-rich dacite that probably represents an older ignimbrite. It seems likely that in the heavy mineral separate of bulk Tocanao ignimbrite xenocrystic grains derived from the crystal-rich lithic clasts dominate the zircon population.

Ion microprobe U–Pb measurements of xenocrysts from the Toconao bulk ignimbrite sample are too imprecise to distinguish between a concordant younger growth episode or discordancy due to Pb-loss from older grains. A 13 and 9 Ma

Table 2
Summary of U–Pb zircon ages and other relevant characteristics for Atana and Toconao pumice

| Unit | Description | Locality | Crystals | w.r. $SiO_2$ | m.g. $SiO_2$ | Age[a] (Ma) $^{238}U/^{206}Pb$ | MSWD | Age[b] (Ma) $^{238}U/^{206}Pb$ | MSWD | Age[c] (Ma) K/Ar | U–Pb sample |
|---|---|---|---|---|---|---|---|---|---|---|---|
| | | | wt% | wt% | wt% | | | | | | |
| Atana | single pumice | Pampa de Lari | 40 | 69.5 | 77.0 | 4.11 ± 0.20 | 2.6 | 3.96 ± 0.19 | 1.1 | 3.94 ± 0.12<br>4.01 ± 0.11<br>4.11 ± 0.12 | Lari-96h-6 |
| Toconao | composite pumice | Quebrada Toconao | < 3 | 76.8 | 77.6 | 4.65 ± 0.13 | 1.1 | 4.44 ± 0.16 | 0.97 | 5.27 ± 1.12 | Toc-97h-2 |

Concordia intercept ages and $^{204}Pb$-corrected (using values for anthropogenic $^{206}Pb/^{204}Pb$ and $^{207}Pb/^{204}Pb$ from Sañudo-Wilhelmy and Flegal, 1994) ages calculated as described in text. Note that errors (2σ) have been scaled by square-root of MSWD to account for sample heterogeneities and/or unexplained analytical error. Whole-rock (w.r.) and matrix glass (m.g.) compositions (100% volatile-free) and K/Ar ages for samples from the same localities (Lindsay et al., 2001a and Lindsay et al., 2001b) shown for comparison.

[a] Concordia intercept age.

[b] Common Pb-corrected using $^{206}Pb/^{204}Pb = 18.8$ and $^{207}Pb/^{204}Pb = 15.4$.

[c] The three ages for Lari-96h-6 represent different aliquots of the biotite separate; Toconao age is from biotites of composite pumice sample Toc-97h-3 from same location as Toc-97h-2.

(over-) growth period, however, seems likely, since (1) diffusive Pb exchange between zircon and melt (Cherniak and Watson, 2000) is insignificant at temperatures inferred for the Atana magma (~780° C, Lindsay et al., 2001b), (2) sharp boundaries between older cores and younger rims are visible in CL images (Fig. 2A), (3) rhyolitic melt inclusions are present in 13 Ma grains and (4) core and rim analyses of another grain yielded overlapping Proterozoic ages, which precludes that all rims are affected by Pb-loss (Fig. 2B).

Based on these considerations, three populations of xenocrystic zircons can be identified: (1) Proterozoic–Ordovician individual grains or relict cores, (2) ~13-Ma grains and overgrowth zones, and (3) ~9-Ma grains. The latter age agrees well with K–Ar biotite ages of 9.29–9.44 Ma (Lindsay et al., 2001a) from the Antigua Múcar ignimbrite that directly underlies the Toconao in proximal outcrops both east and west of La Pacana caldera. No ~13-Ma ages, however, have been reported for the central APVC prior to this study. The euhedral textures of the zircon crystals (Fig. 2A) suggest a local magmatic origin without further sedimentary transport. The ~13-Ma ages therefore indicate that the onset of felsic magmatism in this region might have occurred ~3 Ma earlier than previously thought (c.f. de Silva, 1989b).

An important observation is the lack of zircon xenocrysts or xenocrystic cores in Toconao and Atana pumice although we looked for zonations by CL imaging, and, in the Tocanao case, mounted and analyzed all zircons present in the mineral separate. The Sr and Nd isotopic compositions of Toconao, Atana and other APVC ignimbrites suggest a dominantly crustal origin for the magmas (Hawkesworth et al., 1982; Ort et al., 1996; Schmitt et al., 2001; Lindsay et al., 2001b) and the lack of inherited zircon grains implies that either the crustal source was zircon-poor or that the ignimbrite magmas were sufficiently hot to allow complete dissolution of source-rock zircons in the magma. The first explanation is unlikely because geologic studies of the pre-Cenozoic basement in the Central Andes preclude abundant mafic crustal rocks (Lucassen et al., 2001), and such source rocks would also be inconsistent with the radiogenic Sr and non-radiogenic Nd isotope ratios of the APVC magmas. Therefore, our favored explanation for the lack of inheritance in the Toconao and Atana pumices is that restitic zircons were dissolved. The range of Zr concentrations in felsic gneisses and granitoids from the Central Andes is 170–200 ppm according to compilations by Lucassen et al. (2001). Pre-eruptive temperature estimates from two-oxide and two-feldspar thermometry are 770–790°C for the Atana and 730–760°C for the Toconao ignimbrites (Lindsay et al., 2001b). The zircon concentration in sample Lari-96h-6 is ~170 ppm (Lindsay et al., 2001b), close to the satura-

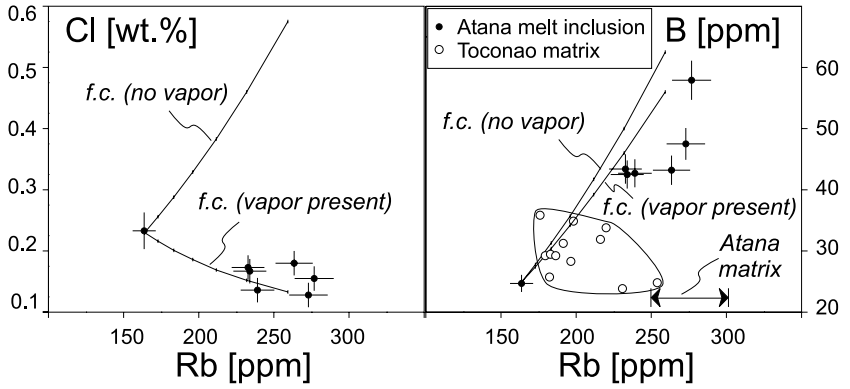


Fig. 4. Cl vs. Rb and B vs. Rb variations of Atana melt inclusion and Toconao matrix glass compositions. Arrows indicate range for Rb in Atana matrix glass. Rb contents of evolved Atana melt inclusions and matrix glasses exceed those of Toconao glasses, which require continued fractionation of the former after separation of the Toconao melt (see text). Variations in melt inclusion volatile contents for Atana can only be explained by vapor-present fractional crystallization (f. c.). Rayleigh fractionation curves were drawn for crystallization between 0 and 50% using a low-Rb melt inclusion as parental melt. Vapor-present fractionation trends were calculated according to Candela (1986) using the following mineral-melt $D$ values: Rb = 0.5 (Lindsay et al., 2001b) and vapor-melt $D$ values: Cl = 40 (Stix and Layne, 1996); B = 3 (Palmer and Swihart, 1996); all others $D$ values = 0; initial melt $H_2O$ content = 4 wt%.

tion concentration of about 150–200 ppm for a magma of Atana dacite composition at these temperature conditions (Watson and Harrison, 1983). For crystal-poor Toconao pumices (~70 ppm Zr), the zircon-saturation temperature also overlaps with the pre-eruptive temperature estimates (Lindsay et al., 2001b). For a crystal-rich dacitic parental magma (Atana pumice is 40–50% crystalline) the liquidus temperature must considerably exceed the pre-eruptive mineral thermometry estimates, and additional heat is expected from admixture of arc andesites in the source region (de Silva, 1989a; Schmitt et al., 2001). Therefore initial undersaturation and dissolution of most restitic zircon is reasonable.

## 7. Conclusions

We obtained apparent U–Pb ages of 4.11 ± 0.20 Ma and 4.65 ± 0.13 Ma (weighted average; 2σ error) from zircon crystals in dacitic (Atana) and rhyolitic (Toconao) ignimbrites, respectively. Both ignimbrites erupted from La Pacana caldera. The U–Pb zircon ages overlap with K–Ar biotite ages of ~4.0 Ma for the caldera-forming Atana eruption. Variations in Rb and other incompatible trace elements demonstrate that differentiation of both the Atana and the Toconao magmas must have continued after separation in a stratified rhyolite-over-dacite system and the slightly older U–Pb zircon ages from Toconao pumice indicate that zircon crystallized in the La Pacana magma system over a time-span of several 100 kyr prior to eruption. The chronostratigraphic data are consistent with chemical evidence that the crystal-poor Toconao rhyolite is derived from a crystal-rich dacitic parental magma. Gas-driven filter pressing might have facilitated melt segregation from the volatile-saturated and crystal-rich dacitic magma into a cupola of the storage reservoir. Finally, the presence of ~13-Ma xenocrystic zircons found in a Toconao bulk ignimbrite sample defines a new limit for the onset of felsic magmatism in the central part of the APVC.

## Acknowledgements

We thank M. Gardeweg, formerly Sernageomin, Chile, and the staff at the Universidad Católica del Norte in Antofagasta, in particular H. Wilke, for advice and support during field work. We also thank the members of the UCLA ion

probe group, C. Coath, K. McKeegan, M. Grove and G. Jarzebinski. M. Harrison and J. Vazquez are thanked for insightful discussions and helpful comments on an earlier version of the manuscript. Funding was provided by DoE Grant to UCLA (4-443875-MH-22 400) and the SFB267 of the Deutsche Forschungsgemeinschaft. C.R. Bacon and M.H. Ort are thanked for their reviews as is M.T. Mangan for editorial handling.

## References

Baldwin, S.L., Ireland, T.R., 1995. A tale of two eras: Pliocene–Pleistocene unroofing of Cenozoic and late Archean zircons from active metamorphic core complexes, Solomon Sea, Papua New Guinea. Geology 23, 1023–1026.

Brown, S.J.A., Fletcher, I.R., 1999. SHRIMP U-Pb dating of pre-eruption growth history of zircons from the 340 ka Whakamaru Ignimbrite, New Zealand: evidence for >250 k.y. magma residence times. Geology 27, 1035–1038.

Candela, P.A., 1986. Toward a thermodynamic model for the halogens in magmatic systems: an application to melt-vapor-apatite equilibria. Chem. Geol. 57, 289–301.

Cherniak, D.J., Watson, E.B., 2000. Pb diffusion in zircon. Chem. Geol. 172, 5–24.

Chmielowski, J., Zandt, G., Haberland, C., 1999. The central Andean Altiplano-Puna magma body. Geophys. Res. Lett. 26, 783–786.

Christensen, J.N., Halliday, A.N., 1996. Rb-Sr ages and Nd isotopic composition of melt inclusions from the Bishop tuff and the generation of silcic magma. Earth Planet. Sci. Lett. 144, 547–561.

Dalrymple, G.B., Grove, M., Lovera, O.M., Harrison, T.M., Hulen, J.B., Lanphere, M.A., 1999. Age and thermal history of The Geysers plutonic complex (felsite unit), Geysers geothermal field, California; a $^{40}Ar/^{39}Ar$ and U-Pb study. Earth Planet. Sci. Lett. 30, 285–298.

de Silva, S.L., 1989a. Altiplano-Puna volcanic complex of the central Andes. Geology 17, 1102–1106.

de Silva, S.L., 1989b. Geochronology and stratigraphy of the ignimbrites from the 21°30′ S to 23°30′ S portion of the central Andes of northern Chile. J. Volcanol. Geotherm. Res. 37, 93–131.

de Silva, S.L., 2001. Comment on 'Magmas in collision: rethinking chemical zonation in silicic magmas: by Eichelberger et al.'. Geology 29, 1063–1064.

Eichelberger, J.C., Chertkoff, D.G., Dreher, S.T., Nye, C.J., 2000. Magmas in collision: rethinking chemical zonation in silicic magmas. Geology 28, 603–606.

Eichelberger, J.C., Izbekov, P., 2000. Eruption of andesite triggered by dike injection: contrasting cases at Karymsky Volcano, Kamchatka and Mount Katmai, Alaska. R. Soc. London Philos. Trans. Ser. A. 358, 1465–1485.

Eichelberger, J.C., Chertkoff, D.G., Dreher, S.T., Nye, C.J., 2001. Reply to Comment on 'Magmas in collision: rethinking chemical zonation in silicic magmas'. Geology 29, 1063–1064.

Francis, P.W., Baker, M.C.W., 1978. Sources of two large ignimbrites in the central Andes; some Landsat evidence. J. Volcanol. Geotherm. Res. 4, 81–87.

Gardeweg, M., Ramírez, C.F., 1987. La Pacana Caldera and the Atana Ignimbrite; a major ash-flow and resurgent caldera complex in the Andes of northern Chile. Bull. Volcanol. 49, 547–566.

Grove, M., Harrison, T.M., 1999. Monazite Th-Pb age depth profiling. Geology 27, 487–490.

Haberland, C., Rietbrock, A., 2001. Attenuation tomography in the western central Andes: a detailed insight into the structure of a magmatic arc. J. Geophys. Res. 106, 11151–11167.

Hawkesworth, C.J., Hammill, M., Gledhill, A.R., van Calsteren, P., Rogers, G., 1982. Isotope and trace element evidence for late-stage intra-crustal melting in the High Andes. Earth Planet. Sci. Lett. 58, 240–254.

Hildreth, W., 1981. Gradients in silicic magma chambers; implications for lithospheric magmatism. J. Geophys. Res. 86, 10153–10192.

Housh, T.B., Luhr, J.F., 1991. Plagioclase-melt equilibria in hydrous systems. Am. Mineral. 76, 477–492.

Lindsay, J.M., de Silva, S., Trumbull, R., Emmermann, R., Wemmer, K., 2001a. La Pacana caldera, N. Chile: a re-evaluation of the stratigraphy and volcanology of one of the world's largest resurgent calderas. J. Volcanol. Geotherm. Res. 106, 145–173.

Lindsay, J.M., Schmitt, A.K., Trumbull, R.B., de Silva, S.L., Siebel, W., Emmermann, R., 2001b. Magmatic evolution of the La Pacana Caldera system, central Andes, Chile: compositional variation of two cogenetic, large-volume felsic ignimbrites and implications for contrasting eruption mechanisms. J. Petrol. 42, 459–486.

Lucassen, F., Becchio, R., Harmon, R., Kasemann, S., Franz, G., Trumbull, R., Romer, R.L., Dulski, P., 2001. Composition and density model of the continental crust in an active continental margin - the Central Andes between 18° and 27°S. Tectonophysics 341, 195–223.

Mattinson, J.M., 1973. Anomalous isotopic composition of lead in young zircons. Carnegie Inst. Washington Year B. 72, 613–616.

Ort, M.H., 1993. Eruptive processes and caldera formation in a nested downsag-collapse caldera, Cerro Panizos, central Andean mountains. J. Volcanol. Geotherm. Res. 56, 221–252.

Ort, M.H., Coira, B.L., Mazzoni, M.M., 1996. Generation of a crust-mantle magma mixture; magma sources and contamination at Cerro Panizos central Andes. Contrib. Mineral. Petrol. 123, 308–322.

Palmer, M.R., Swihart, G.H., 1996. Boron isotope geochemistry: an overview. In: Grew, E.S., Anovitz, L.M. (Eds.), Boron: Mineralogy, Petrology and Geochemistry. Reviews in Mineralogy 33, Mineralogical Society of America, Washington, DC, pp. 709–744.

Paces, J.B., Miller, J.D., 1993. Precise U-Pb ages of Duluth Complex and related mafic intrusions, northeastern Minnesota; geochronological insights to physical, petrogenetic, paleomagnetic, and tectonomagnetic processes associated with the 1.1 Ga Midcontinent Rift System. J. Geophys. Res. 98, 13997–14013.

Reid, M.R., Coath, C.D., 2000. In situ U-Pb ages of zircons from the Bishop Tuff; no evidence for long crystal residence times. Geology 28, 443–446.

Sañudo-Wilhelmy, S.A., Flegal, A.R., 1994. Temporal variations in lead concentrations and isotopic composition in the Southern California Bight. Geochim. Cosmochim. Acta 58, 3315–3320.

Schärer, U., 1984. The effect of initial $^{230}$Th disequilibrium on young U-Pb ages: the Makalu case, Himalaya. Earth Planet. Sci. Lett. 67, 191–204.

Schmitt, A.K., de Silva, S.L., Trumbull, R.B., Emmermann, R., 2001. Magma evolution in the Purico ignimbrite complex, N. Chile: Evidence for zoning of a dacitic magma by injection of rhyolitic melts following mafic recharge. Contrib. Mineral. Petrol. 140, 680–700.

Sisson, T.W., Bacon, C.R., 1999. Gas-driven filter pressing in magmas. Geology 27, 613–616.

Smith, R.L., 1979. Ash-flow magmatism. In: Chapin, C.E., Elston, W.E. (Eds.), Ash-flow Tuffs. Geological Society of America Special Paper 180. Geological Society of America, Boulder, CO, pp. 5–27.

Stix, J., Layne, G.D., 1996. Gas saturation and evolution of volatile and light lithophile elements in the Bandelier magma chamber between two caldera-forming eruptions. J. Geophys. Res. 101, 25181–25196.

Tamic, N., Behrens, H., Holtz, F., 2001. The solubility of $H_2O$ and $CO_2$ in rhyolitic melts in equilibrium with a mixed $CO_2$-$H_2O$ fluid phase. Chem. Geol. 174, 333–347.

van den Bogaard, P., Schirnick, C., 1995. $^{40}$Ar/$^{39}$Ar laser probe ages of Bishop Tuff quartz phenocrysts substantiate long-lived silicic magma chamber at Long Valley, United States. Geology 23, 759–762.

Watson, E.B., Harrison, T.M., 1983. Zircon saturation revisited; temperature and composition effects in a variety of crustal magma types. Earth Planet. Sci. Lett. 64, 295–304.